Chemical Solvent in Chemical Solvent: A Class of Hybrid Materials for Effective Capture of CO_2

Feng-Feng Chen
Key Laboratory of Poyang Lake Environment and Resource Utilization of Ministry of Education, School of Resources Environmental and Chemical Engineering, Nanchang University, Nanchang, Jiangxi 330031, P. R. China

College of Chemistry and Chemical Engineering, Jiangxi Normal University, Nanchang, Jiangxi 330022, P. R. China

Kuan Huang and Jie-Ping Fan
Key Laboratory of Poyang Lake Environment and Resource Utilization of Ministry of Education, School of Resources Environmental and Chemical Engineering, Nanchang University, Nanchang, Jiangxi 330031, P. R. China

Duan-Jian Tao
College of Chemistry and Chemical Engineering, Jiangxi Normal University, Nanchang, Jiangxi 330022, P. R. China

DOI 10.1002/aic.15952
Published online September 12, 2017 in Wiley Online Library (wileyonlinelibrary.com)

Amino acid ionic liquids (AAILs) are chemical solvents with high reactivity to CO_2. However, they suffer from drastic increase in viscosity on the reaction with CO_2, which significantly limits their application in the industrial capture of CO_2. In this work, 1-ethyl-3-methylimidazolium acetate ([emim][Ac]) which also exhibits chemical affinity to CO_2 but low viscosity, and its viscosity does not increase drastically after CO_2 absorption, was proposed as the diluent for AAILs to fabricate hybrid materials. The AAIL+[emim][Ac] hybrids were found to display enhanced kinetics for CO_2 absorption, and their viscosity increase after CO_2 absorption are much less significant than pure AAILs. More importantly, owing to the fact that [emim][Ac] itself can absorb large amount of CO_2, the AAIL+[emim][Ac] hybrids still have high absolute capacities of CO_2. Such hybrid materials consisting of a chemical solvent plus another chemical solvent are believed to be a class of effective absorbents for CO_2 capture. © 2017 American Institute of Chemical Engineers *AIChE J*, 64: 632–639, 2018

Keywords: ionic liquids, chemical solvents, hybrid materials, CO_2 capture, absolute capacity

Introduction

The capture of CO_2 has attracted growing interests across chemical industry in the past decades, as a solution to "greenhouse effect" which may pose destructive impacts on the environment and eco-system.[1] The major source of CO_2 emission is flue gas resulting from the burning of fossil fuels. As the content of CO_2 in flue gas is low (ca. 10–20 v/v%),[2] the capture of CO_2 from flue gas requires solvents with chemical affinity to CO_2. Organic amines (either in aqueous or organic solutions) are the most widely used absorbents for CO_2 capture in industrial processes because of their low cost, high capacity and fast kinetics.[3] However, organic amines are accompanied with some inherent drawbacks, such as high volatility, strong corrosion, and intensive energy demand for regeneration. Therefore, it is of significance to develop new absorbents, from the viewpoint of green and sustainable chemistry, for CO_2 capture.

Ionic liquids (ILs) are regarded as potential substitutes to conventional solvents for CO_2 capture, owing to their unique characteristics including negligible volatility, wide liquid range, high thermal stability, and tunable physicochemical properties.[4–6] To date, a wide range of ILs with chemical reactivity to CO_2 have been specifically designed, for example acetate-based ILs,[7–9] amine-functionalized ILs,[10–13] ILs with aprotic heterocyclic anions,[14–17] and phenolic ILs.[18] As a subcategory of amine-functionalized ILs, amino acid ionic liquids (AAILs) are particularly promising because of the low cost, abundant availability, and nontoxic biodegradability of amino acids.[19] Depending on the electronic environment of amino acid anions, the absorption of CO_2 in AAILs is subjected to carbamate mechanism or carbamic acid mechanism.[11,12] Correspondingly, the absorption capacity of CO_2 in AAILs can reach ~0.5 mol/mol or ~1.0 mol/mol theoretically. Unfortunately, AAILs suffer from drastic increase in viscosity upon the reaction with CO_2, mainly due to the formation of complex

Correspondence concerning this article should be addressed to K. Huang at kuan.huang@yahoo.com or Duan-Jian Tao at djtao@jxnu.edu.cn.

hydrogen-bond networks.[20] This fact renders significant diffusion barrier for the absorption of CO_2 in AAILs, and extra energy is required for the transportation of CO_2-loaded AAILs. As a consequence, it is a challenge to directly employing pure AAILs for CO_2 capture in the industry.

Diluting AAILs with low-viscous physical solvents or immobilizing AAILs in porous supports, represent two commonly referred strategies to promote the absorption of CO_2 in AAILs. For example, Han et al.[21] and Deng et al.[22] blended choline prolinate ([Ch][Pro]) and tetrabutylphosphonium glycinate ([P_{4444}][Gly]) respectively, with polyethylene glycol (PEG) for reversible absorption of CO_2; Wu et al.,[23] Zhou et al.,[24,25] Li et al.[26] and Luo et al.[27,28] investigated the absorption of CO_2 in aqueous solutions of AAILs, such as tetramethylammonium glycinate ([N_{1111}][Gly]), 1-(2-hydroxlethyl)-3-methylimidazolium glycinate ([C_2OHmim][Gly], 1-ethyl-3-methylimidazolium glycinate ([emim][Gly]), etc.; Li et al.[29,30] immobilized 1-ethyl-3-methylimidazolium glycinate ([emim][Gly]) and 1-ethyl-3-methylimidazolium lysinate ([emim][Lys]) in porous poly(methyl methacrylate) (PMMA) microspheres for facilitated adsorption of CO_2. These efforts demonstrated that the kinetics of CO_2 absorption in hybrids of AAILs with physical solvents or AAILs with porous supports is significantly enhanced in relative to that in pure AAILs. In addition, the issue associated with the transportation of highly viscous CO_2-loaded AAILs is avoided.

However, the inert nature of physical solvents and porous supports inevitably causes the sacrifice of absolute capacity of CO_2 (e.g., in terms of mol/kg or g/g) in absorbents. In addition, the volatile nature of physical solvents mentioned above (e.g., water) diminishes the advantage of ILs as nonvolatile solvents. In this work, we proposed to use 1-ethyl-3-methylimidazolium acetate ([emim][Ac]) as the diluent for AAILs, to construct completely nonvolatile materials that not only enable rapid absorption of CO_2, but also exhibit high absolute capacity of CO_2. [emim][Ac] has been previously identified as a solvent with chemical affinity to CO_2 through the formation of carbene-CO_2 adducts.[31] More importantly, [emim][Ac] is with low viscosity and its viscosity does not show drastic increase after the absorption of CO_2.[31] Dissolving AAILs in [emim][Ac] can promote the absorption of CO_2 in AAILs, meanwhile, maintain the overall high absolute capacity of CO_2 in absorbents. Such hybrid materials, consisting of a chemical solvent plus another chemical solvent, are very scarce in the literature to the best of our knowledge and expected to be a class of promising absorbents for CO_2 capture.

Experimental

Materials

CO_2 (99.99 v/v%) was purchased from Jiangxi Jingong Special Gas Co., Ltd. 1-Ethyl-3-methylimidazolium chlorine ([emim][Cl], 99 wt %) was purchased from the Centre of Green Chemistry and Catalysis, Lanzhou Institute of Chemical Physics, Chinese Academy of Sciences. Glycine (99 wt %), L-alanine (99 wt %) and acetic acid (99 wt %) were supplied by J&K Scientific Ltd. Dowex Monosphere 550A (OH form) anion exchange resin was supplied by Dow Chemical Co. Ltd. All chemicals were used directly without any further purification.

Synthesis

1-Ethyl-3-methylimidazolium glycinate ([emim][Gly]), 1-ethyl-3-methylimidazolium alaninate ([emim][Ala]) and 1-ethyl-3-methylimidazolium acetate ([emim][Ac]) were prepared by a two-step route in the first step, an aqueous solution of 1-ethyl-3-methylimidazolium hydroxide ([emim][OH]) was prepared by passing [emim][Cl] through the Dowex Monosphere 550A (OH form) anion exchange resin. In the second step, equimolar glycine, L-alanine or acetic acid was added to the aqueous solution of [emim][OH], and the mixture was stirred at room temperature for 12 h. Most of the water was removed by rotary evaporation at 333.2 K. The resulting liquid was further dried under vacuum at 353.2 K for 48 h. [emim][Gly], [emim][Ala] and [emim][Ac] were finally obtained as pale-yellow liquids. The water contents in synthesized ILs were determined to be less than 100 ppm by Karl Fischer titration (Metrohm 756 KF coulometer). The chloride residues in synthesized ILs were determined to be less than 0.05 wt % by Mohr titration.

AAIL+[emim][Ac] hybrid materials were prepared by directly mixing [emim][Gly] or [emim][Ala] with [emim][Ac]. The molar ratios of [emim][Gly]:[emim][Ac] and [emim][Ala]:[emim][Ac] in hybrid materials are set to 1:1 in this work.

Characterizations

^{1}H NMR and ^{13}C NMR spectra were recorded on Bruker Ascend 400 MHz spectrometer with TMS as the internal standard. ATR-FTIR spectra were recorded on NEXUS870 FT-IR spectrometer. Elemental analysis (EA) was performed on Elementar Vario El III. Thermogravimetric analysis (TGA) were performed on PerkinElmer Diamond from room temperature to 873.2 K at a heating rate of 10 K/min under flowing N_2.

The densities were measured on Anton Paar DMA 5000 densiometer with a precision of 0.00001 g/cm^3. The viscosities were measured on Brookfield DV II+ Pro viscometer with an uncertainty of $\pm 1\%$ in relation to the full scale.

Measurement of CO_2 absorption

The apparatus for measuring CO_2 absorption is the same as that reported in our previous work.[32] The whole device consists of two 316 L stainless steel chambers whose volumes are 128.47 cm^3 (V_1) and 49.67 cm^3 (V_2), respectively. The bigger chamber, used as gas reservoir, isolates the gas before it contacts with the absorbents in the smaller chamber. The smaller chamber, named as equilibrium cell, is equipped with a magnetic stirrer. The temperatures (T) of both chambers are controlled using a water bath with an uncertainty of ± 0.1 K. The pressures in two chambers are monitored using two pressure transducers with an uncertainty of $\pm 0.2\%$ (in relation to the full scale). The pressure transducers are connected to a numeric instrument to record the pressure changes online. In a typical run, a known mass (w) of absorbent was placed into the equilibrium cell, and the air in two chambers was evacuated. The remaining pressure in equilibrium cell was recorded to be P_0 (<0.001 bar). The gas from cylinder was then fed into the gas reservior to a pressure of P_1. The needle valve between the two chambers was turned on to let the gas be introduced to the equilibrium cell. Absorption equilibrium was thought to be reached when the pressures of two chambers remained constant for at least 2 h. The equilibrium pressures were denoted as P_2 for the equilibrium cell and P'_1 for the gas reservoir. The gas partial pressure in the equilibrium cell was $P_g = P_2 - P_0$. The gas uptake, $n(P_g)$, can thus be calculated using Eq. 1

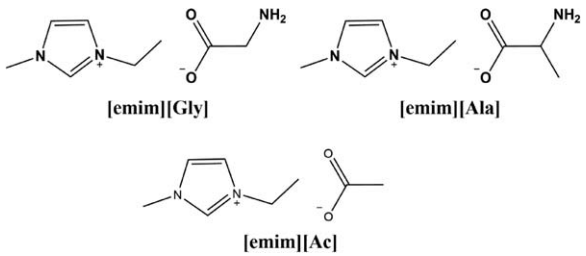

Scheme 1. Chemical structures of ILs synthesized in this work.

$$n(P_g) = \rho_g(P_1, T)V_1 - \rho_g(P_1', T)V_1 - \rho_g(P_g, T)(V_2 - w/\rho_{IL}) \quad (1)$$

where ρ_g (P_i, T) represents the density of gas in mol/cm^3 at P_i ($i = 1, g$) and T. ρ_{IL} is the density of IL in g/cm^3 at T. V_1 and V_2 represent the volumes in cm^3 of two chambers, respectively. Continual measurements of solubility data at elevated pressures were performed by introducing more gas into the equilibrium cell to reach new equilibrium. The solubility of gas was defined in terms of mol gas/kg absorbent in this work. Duplicate experiments were run for each IL to obtain averaged values of gas solubility. The reproducibility of solubility data in this work was well within ±1%.

Results and Discussion

Structural characterizations

Three ILs ([emim][Gly], [emim][Ala] and [emim][Ac]) were synthesized in this work, and their chemical structures are shown in Scheme 1. The structures of synthesized ILs were characterized by ^{1}H NMR spectra, ^{13}C NMR spectra, FTIR spectra, EA, and TGA. See the following for characterization results:

[emim][Gly] ^{1}H NMR (400 MHz, DMSO, 298.2K, TMS), δ (ppm): 1.41 (3H, t), 2.81 (2H, d), 3.90 (3H, s), 4.21 (2H, m), 7.86 (1H, s), 7.96 (1H, s), 10.09 (1H, s); ^{13}C NMR (101 MHz, DMSO, 298.2K, TMS), δ (ppm): 15.6, 35.9, 44.4, 46.6, 122.4, 123.9, 137.9, 175.4; FTIR, $\bar{\nu}$ (cm^{-1}): 701, 821, 871, 1019, 1091, 1175, 1334, 1386, 1452, 1574, 2979, 3063, 3355; EA, calculated for $C_8H_{15}N_3O_2$: C 51.88%, N 22.69%, H 8.16%, found: C 51.26%, N 22.41%, H 8.06%; TGA, decomposition temperature: 464 K.

[emim][Ala] ^{1}H NMR (400 MHz, DMSO, 298.2K, TMS), δ (ppm): 1.39 (3H, t),1.94 (3H, m), 2.58 (1H, m), 3.91 (3H, m), 4.25 (2H, m), 7.89 (1H, s),7.98 (1H, s), 10.31 (1H, s); ^{13}C NMR (101 MHz, DMSO, 298.2K, TMS), δ (ppm): 15.7, 35.9, 43.0, 44.3, 122.4, 123.9, 138.2, 175.3; FTIR, $\bar{\nu}$ (cm^{-1}): 701, 773, 893, 934, 1019, 1080, 1130, 1178, 1307, 1348, 1393, 1455, 1575, 2867, 2960, 3054, 3347; EA, calculated for $C_9H_{17}N_3O_2$: C 54.25%, N 21.09%, H 8.60%, found: C 53.86%, N 20.94%, H 8.54%; TGA, decomposition temperature: 457 K.

[emim][Ace] ^{1}H NMR (400 MHz, DMSO, 298.2K, TMS), δ (ppm): 1.40 (3H, dt), 1.61 (3H, s), 3.96 (3H, d), 4.26 (2H, q), 7.90 (1H, d), 8.01 (1H, d), 10.32 (1H, s,); ^{13}C NMR (101 MHz, DMSO, 298.2K, TMS), δ (ppm): 15.6, 26.6, 35.8, 44.3, 122.4, 123.9, 138.3, 173.7; FTIR, $\bar{\nu}$ (cm^{-1}): 701, 806, 898, 1001, 1091, 1181, 1256, 1325, 1383, 1427, 1583, 1667, 2873, 2977, 3033; EA, calculated for $C_8H_{14}N_2O_2$: C 56.45%, N 16.46%, H 8.29%, found: C 56.07%, N 16.35%, H 8.23%; TGA, decomposition temperature: 490 K.

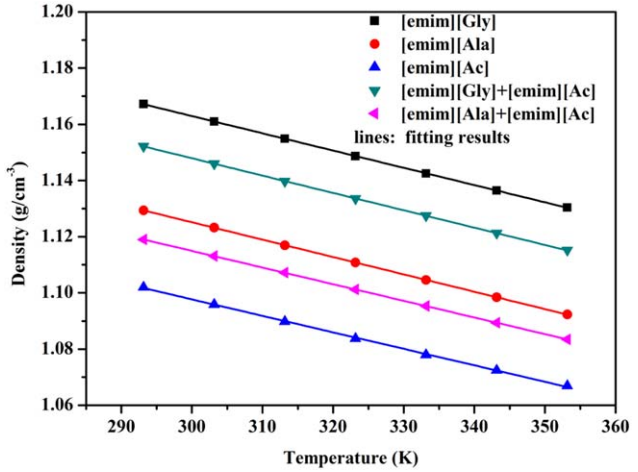

Figure 1. Densities of pure ILs and hybrid materials.

[Color figure can be viewed at wileyonlinelibrary.com]

Two hybrid materials ([emim][Gly]+[emim][Ac] and [emim][Ala]+[emim][Ac]) were prepared in this work, and their stability were evaluated by TGA:

[emim][Gly]+[emim][Ac] TGA, decomposition temperature: 474 K.

[emim][Ala]+[emim][Ac] TGA, decomposition temperature: 472 K.

Physical properties

Densities and viscosities are fundamental data of absorbents and very important for the design of CO_2 capture process. Figure 1 shows the densities of pure ILs and AAIL+[emim][Ac] hybrid materials at different temperatures. The densities of three pure ILs follow the sequence of [emim][Gly] > [emim][Ala] > [emim][Ac]. The densities of [emim][Gly]+[emim][Ac] are smaller than those of [emim][Gly] but larger than those of [emim][Ac], meanwhile, the densities of [emim][Ala]-[emim][Ac] are smaller than those of [emim][Ala] but larger than those of [emim][Ac]. Figure 2 shows the viscosities of pure ILs and AAIL+[emim][Ac] hybrid materials at different temperatures. The viscosities of three pure ILs also follow the sequence of [emim][Gly] > [emim][Ala] > [emim][Ac]. The viscosities of [emim][Gly]+[emim][Ac] are lower than those of [emim][Gly]

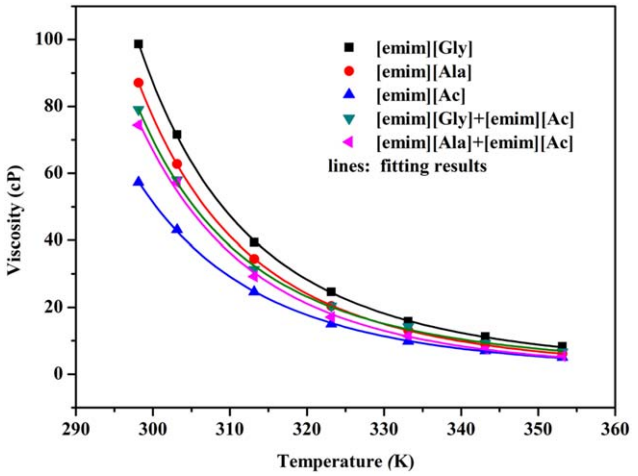

Figure 2. Viscosities of pure ILs and hybrid materials.

[Color figure can be viewed at wileyonlinelibrary.com]

Table 1. Fitted Parameters of Eqs. 2 and 3

Parameters	[emim][Gly]	[emim][Ala]	[emim][Ac]	[emim][Gly] + [emim][Ac]	[emim][Ala] + [emim][Ac]
A_1	1.35	1.31	1.27	1.33	1.29
$A_2\times10^4$	−6.14	−6.18	−5.87	−6.17	−5.92
η_0	0.0601	0.0116	0.00635	0.0815	0.00255
D	795	1158	1341	690	1591
T_0	191	168	151	198	144

but higher than those of [emim][Ac], meanwhile, the viscosities of [emim][Ala]+[emim][Ac] are lower than those of [emim][Ala] but higher than those of [emim][Ac]. The viscosities of [emim][Gly]+[emim][Ac] and [emim][Ala]+[emim][Ac] are determined to be 79.1 and 74.4 cP, respectively, at 298.2 K, being higher than those of AAILs + H_2O hybrids[23,27,28] but lower than those of AAILs + PEG hybrids.[22]

Furthermore, the densities of pure ILs and AAIL+[emim][Ac] hybrid materials decrease linearly with the increase of temperature, while the viscosities decrease nonlinearly with the increase of temperature. The densities and viscosities can be correlated with Eqs. 2 and 3, respectively.[33]

$$\rho=A_1+A_2T \tag{2}$$

$$\eta=\eta_0\cdot\exp\left(\frac{D}{T-T_0}\right) \tag{3}$$

In Eqs. 2 and 3, ρ is the density in cm^3/g, η is the viscosity in cP, T is the temperature in K, A_1, A_2, η_0, D, and T_0 are empirical parameters. Fitting results are shown in Figures 1 and 2, and fitted parameters are summarized in Table 1.

CO_2 absorption rate

Figure 3 shows the amount of CO_2 absorbed in pure AAILs and AAIL+[emim][Ac] hybrid materials as a function of absorption time at 313.2 K and 1 bar. As can be seen, the absorption of CO_2 in pure [emim][Gly] and [emim][Ala] are very slow, with the absorption of CO_2 in them still not reaching equilibrium after 3 h. However, the absorption of CO_2 in [emim]Gly]+[emim][Ac] and [emim][Ala]+[emim][Ac] are much more rapid, with the equilibrium time being less than 1 h in them. After 1 h of absorption, the amount of CO_2 absorbed in [emim]Gly]+[emim][Ac] and [emim][Ala]-[emim][Ac] are 2.60 and 2.19 mol/kg, respectively, while those in pure [emim][Gly] and [emim][Ala] are only 2.02 and 1.70 mol/kg, respectively. Therefore, diluting [emim][Gly] and [emim][Ala] with [emim][Ac] can significantly enhance the rate of CO_2 absorption in them.

Viscosity change after CO_2 absorption

Figure 4 shows the viscosities of pure AAILs and AAIL+[emim][Ac] hybrid materials before and after CO_2 absorption at 313.2 K and 1 bar. Obviously, the viscosity increase of [emim]Gly]+[emim][Ac] and [emim][Ala]-[emim][Ac] after CO_2 absorption is much less significant than those of pure [emim][Gly] and [emim][Ala]. For example, the viscosity of [emim]Gly]+[emim][Ac] and [emim][Ala]-[emim][Ac] increase by only 6.7 times (from 31.3 to 240.3 cP) and 53.2 times (from 29.2 to 1584 cP), respectively, after CO_2 absorption. However, the viscosity of pure [emim][Gly] and [emim][Ala] increase by 255 times (from 39.4 to 10097 cP) and 319 times (from 34.5 to 11046 cP), respectively, after CO_2 absorption. The CO_2-loaded [emim][Gly]+[emim][Ac] and [emim][Ala]+[emim][Ac] still have good fluidity, while the CO_2-loaded [emim]Gly] and [emim][Ala] have very poor fluidity. The reason is that [emim][Ac] still has excellent fluidity even after saturated with CO_2. As shown in Figure 4, the viscosity of [emim][Ac] increases only slightly from 24.6 to 40.9 cP after CO_2 absorption. Therefore, diluting [emim][Gly] and [emim][Ala] with [emim][Ac] can effectively suppress the increase in viscosity of them after CO_2 absorption, and thereby extend the applicability of them in the industrial capture of CO_2.

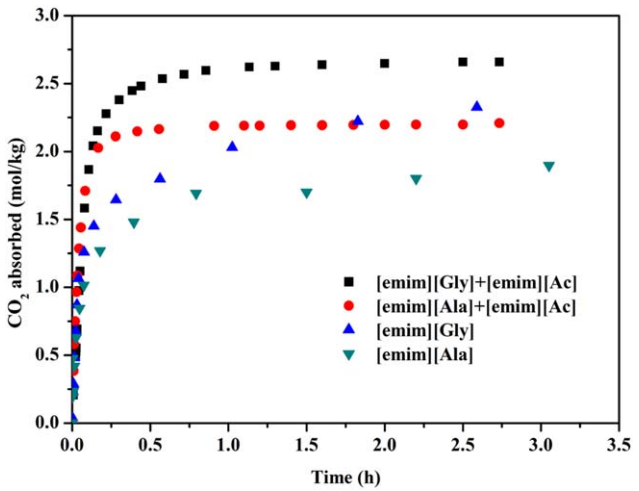

Figure 3. Amount of CO_2 absorbed in pure AAILs and hybrid materials as a function of absorption time at 313.2 K and 1 bar.

[Color figure can be viewed at wileyonlinelibrary.com]

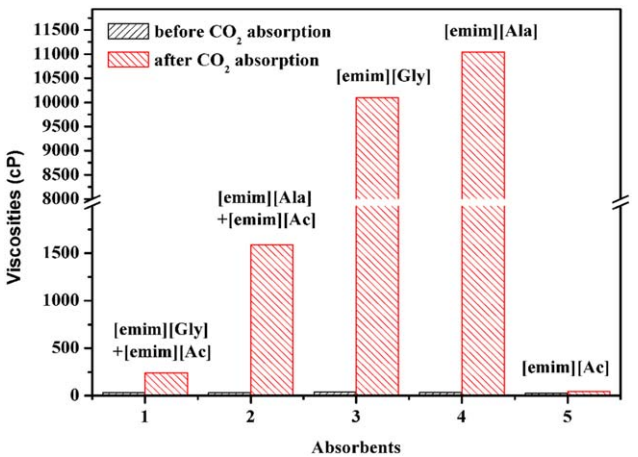

Figure 4. Viscosity change of pure AAILs and hybrid materials after CO_2 absorption at 313.2 K and 1 bar.

[Color figure can be viewed at wileyonlinelibrary.com]

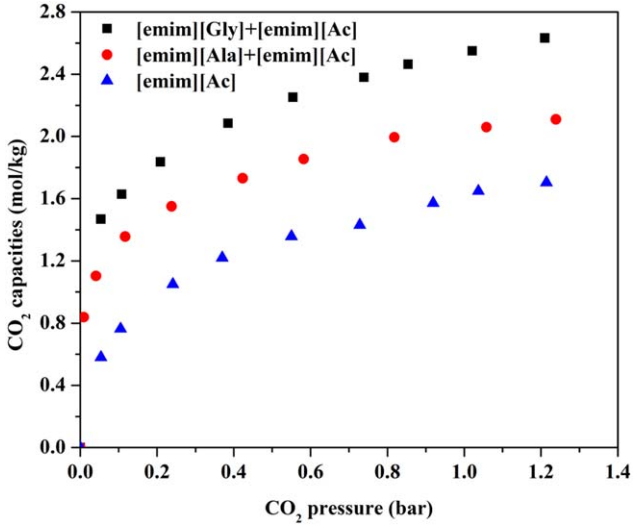

Figure 5. Absorption isotherms of CO_2 in pure [emim][Ac] and hybrid materials at 313.2 K.

[Color figure can be viewed at wileyonlinelibrary.com]

CO_2 absorption capacities

Figure 5 shows the absorption isotherms of CO_2 in pure [emim][Ac] and AAIL+[emim][Ac] hybrid materials at 313.2 K. As pure [emim][Gly] and [emim][Ala] turn to highly viscous gel after CO_2 absorption, the absorption isotherms of CO_2 in them were not determined. Herein, the absorption capacities of CO_2 are defined in terms of mol CO_2/kg absorbent while not mol CO_2/mol IL, because the absolute capacities of CO_2 in absorbents are more concerned in the industry. As can be seen, the CO_2 absorption profiles display nonideality, indicating the chemical absorption of CO_2 in [emim][Gly]-[emim][Ac], [emim][Ala]+[emim][Ac] and [emim][Ac]. Owing to the fact that [emim][Ac] itself can absorb large amount of CO_2 (0.86 mol/kg at 0.15 bar and 1.63 mol/kg at 1 bar), the absorption capacities of CO_2 in [emim][Gly]-[emim][Ac] (1.61 mol/kg at 0.15 bar and 2.54 mol/kg at 1 bar) and [emim][Ala]+[emim][Ac] (1.41 at 0.15 bar and 2.05 mol/kg at 1 bar) still remain at high levels. The absorption

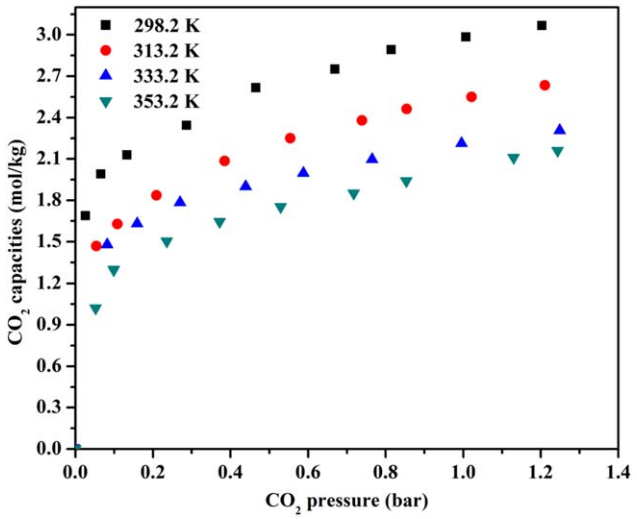

Figure 6. Absorption isotherms of CO_2 in [emim][Gly]-[emim][Ac] at different temperatures.

[Color figure can be viewed at wileyonlinelibrary.com]

Table 2. A Summary of CO_2 Absorption Capacities of Different Absorbents

Absorbents	Temperature (K)	Pressure (bar)	CO_2 Capacity (mol/kg)	Refs.
[emim][Gly]+ [emim][Ac]	298.2	0.15	2.05	This work
	298.2	1	2.98	This work
[emim][Ala]+ [emim][Ac]	313.2	0.15	1.41	This work
	313.2	1	2.05	This work
[emim][Gly]	313.2	0.15	2.29	This work
[emim][Ala]	313.2	1	2.32	This work
	313.2	0.15	1.81	This work
	313.2	1	1.89	This work
[emim][Ac]	313.2	0.15	0.87	This work
	313.2	1	1.65	This work
[Ch][Pro]+PEG_{200}[a]	313.2	0.26	1.02	21
$[C_2(N_{114})_2][Gly]_2$+ H_2O[b]	298.2	1	1.52	23
$[N_{1111}][Gly]+H_2O$[c]	298.2	1	1.62	23
$[C_2OHmim][Gly]+H_2O$[d]	303.2	0.1	0.23	26
$[APmim][Gly]+H_2O$[e]	303.2	1	0.62	25
$DAIL+H_2O$[f]	303.2	1	2.01	35
[DETA][Cl]+EG[g]	303.2	1	2.32	36
$[P_{4444}][Gly]+SiO_2$[h]	318.2	1	0.74	12
$[aP_{4443}][Gly]+SiO_2$[i]	318.2	1	1.38	13
[emim][Lys]+ PMMA[j]	298.2	1	1.82	29
[emim][Gly]+ PMMA[k]	298.2	1	1.71	30
[emim][Ac]	298.2	0.1	1.37	8
$[APbim][BF_4]$	298.2	1	1.82	10
$[P_{66614}]$[2-CNpyr]	295.2	0.15	1.01	14
$[P_{66614}][Pro]$	295.2	0.15	1.56	11
[MTBDH][TFE]	296.2	1	4.32	15
$[P_{66614}][Im]$	296.2	1	1.82	16
$[P_{66614}][PhO]$	303.2	1	1.36	18
$[P_{66614}]$[2-Op]	293.2	0.15	2.33	17
$[P_{4442}]_2$[IDA]	313.2	1	2.95	32
$MEA+H_2O$[l]	298.2	0.1	2.72	37
$MDEA+H_2O$[m]	298.2	0.48	3.29	38

[a]The mass fraction of [Ch][Pro] is 50%.
[b]The mass fraction of $[C_2(N_{114})_2][Gly]_2$ is 40%.
[c]The mass fraction of $[N_{1111}][Gly]_2$ is 40%.
[d]The mass fraction of $[C_2OHmim][Gly]$ is 8%.
[e]The mass fraction of [APmim][Gly] is 11%.
[f]The mass fraction of DAIL is 50%.
[g]The mass fraction of [DETA][Cl] is 36%.
[h]The mass fraction of $[P_{4444}][Gly]$ is 41%.
[i]The mass fraction of $[aP_{4443}][Gly]$ is 41%.
[j]The mass fraction of [emim][Lys] is 49%.
[k]The mass fraction of [emim][Gly] is 50%.
[l]The mass fraction of MEA is 30%.
[m]The mass fraction of MDEA is 50%.

capacities of CO_2 in [emim][Gly]+[emim][Ac] and [emim][Ala]+[emim][Ac] are higher than those in [emim][Ac], because [emim][Gly] and [emim][Ala] exhibit stronger reactivity with CO_2 than [emim][Ac].[9,34] Therefore, [emim][Gly] and [emim][Ala] are the key components while [emim][Ac] is the supporting component for CO_2 absorption in AAIL+[emim][Ac] hybrid materials.

Considering the fast CO_2 absorption rate (equilibrium time <1 h), low viscosities after CO_2 absorption (240.3 cP), and high CO_2 absorptioin capacities (1.61 mol/kg at 0.15 bar and 2.54 mol/kg at 1 bar) of [emim][Gly]+[emim][Ac], it was selected for the investigation of temperature effect on CO_2 absorption capacities. Figure 6 shows the absorption isotherms of CO_2 in [emim][Gly]+[emim][Ac] at different temperatures. As can be seen, the temperature has negative impacts on the

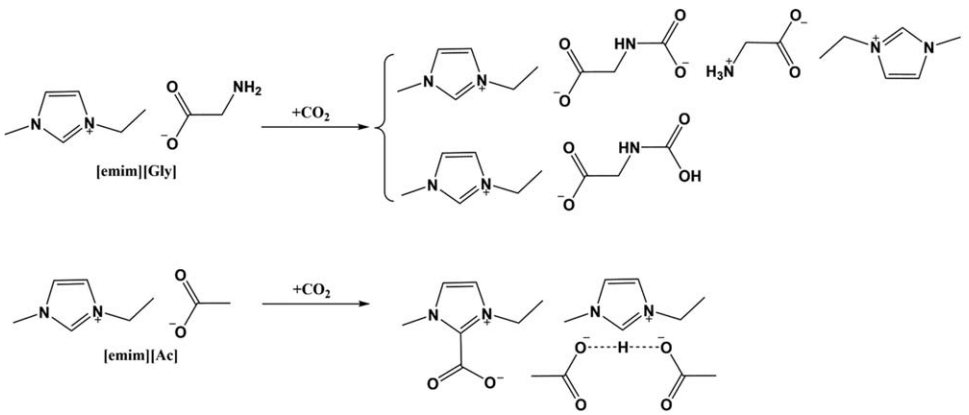

Scheme 2. Mechanism of CO_2 absorption in pure AAILs and pure [emim][Ac].

absorption capacities of CO_2 in [emim][Gly]+[emim][Ac], which is a common phenomenon for gas absorption in liquids.[5] For example, the absorption capacity of CO_2 in [emim][Gly]+[emim][Ac] at 0.15 bar decreases from 2.05 to 1.30 mol/kg, and that at 1 bar decreases from 2.98 to 2.03 mol/kg, as the temperature increases from 298.2 to 353.2 K. Whatever, [emim][Gly]+[emim][Ac] have high absorption capacities of CO_2 even at elevated temperatures, as both components of it exhibit chemical affinity to CO_2.

To thoroughly evaluate the ability of different absorbents for eliminating CO_2 from flue gas, the CO_2 absorption capacities of AAIL+[emim][Ac] hybrid materials and other IL-based hybrids[12,13,21,23,25,26,29,30,35,36] or pure functionalized ILs,[8,10,11,14–18,32] as well as industrially used organic amines,[37,38] are summarized in Table 2. As can be seen, the absorption capacities of CO_2 in AAIL+[emim][Ac] hybrid materials are much higher than those in other IL-based hybrids. From this comparison, the advantage of diluting a chemical solvent with another chemical solvent to fabricate hybrid materials with high absolute capacities of CO_2 is justified. The key is to find a chemical solvent with low viscosity, and its viscosity does not increase drastically after CO_2 absorption. Fortunately, [emim][Ac] is such an ideal candidate. Furthermore, using completely non-volatile [emim][Ac] as the diluent for other chemical solvents can effectively avoid the loss of absorbents, which is a common issue associated with the use of volatile solvents.

The absorption capacities of CO_2 in AAIL+[emim][Ac] hybrid materials also surpass those of most pure functionalized ILs, although are still slightly inferior to those in industrially used organic amines.

Mechanism of CO_2 absorption

The mechanism of CO_2 absorption in pure AAILs and pure [emim][Ac] has been well established.[11,12,31] That is, the reaction of CO_2 with AAILs results in the formation of carbamate or carbamic acid, while the reaction of CO_2 with [emim][Ac] results in the formation of carbene-CO_2 adducts, as shown in Scheme 2. To probe the mechanism of CO_2 absorption in AAIL+[emim][Ac] hybrid materials, ^{13}C NMR spectra of [emim][Gly]+[emim][Ac] before and after CO_2 absorption were collected and shown in Figure 7. As can be seen, four new peaks (141.4, 154.4, 158.0, and 158.6 ppm) are observed in CO_2-loaded [emim][Gly]+[emim][Ac]. The resonances at 141.4 and 154.4 ppm are attributed to the C(2) of imidazole ring and carbonyl in carbene-CO_2 adduct, respectively.[39] The resonances at 158.0 and 158.6 ppm are attributed to the carbonyl in carbamate[10] and carbamic acid, respectively. Furthermore, the resonance of carbonyl in [Ac] shift from 175.9 to 173.0 ppm due to the formation of hydrogen bond between dissociated proton and [Ac]. Therefore, the mechanism of CO_2 absorption in AAIL+[emim][Ac] hybrid materials is generally

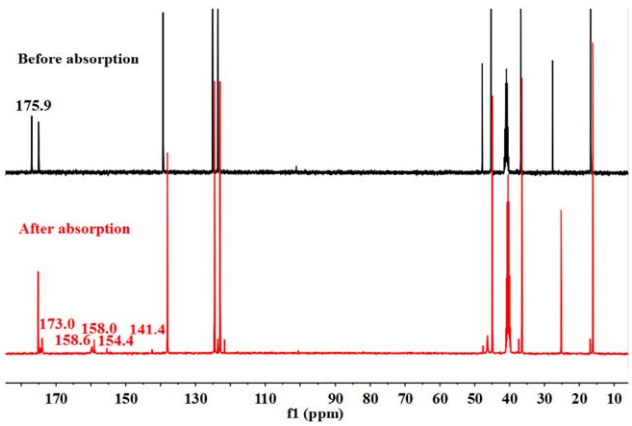

Figure 7. ^{13}C NMR spectra of [emim][Gly]+[emim][Ac] before and after CO_2 absorption.

[Color figure can be viewed at wileyonlinelibrary.com]

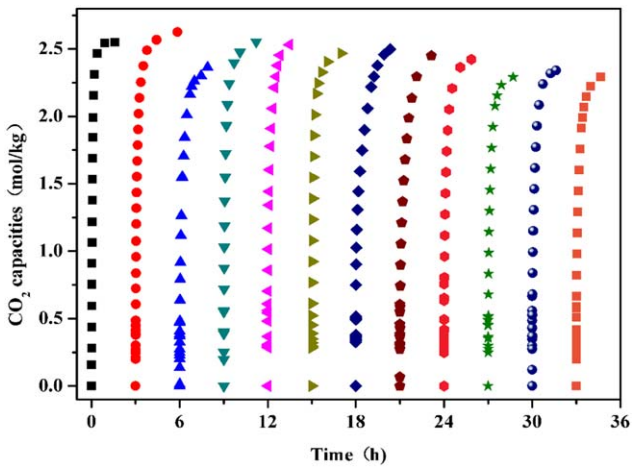

Figure 8. Recyclability of [emim][Gly]+[emim][Ac] for CO_2 absorption.

[Color figure can be viewed at wileyonlinelibrary.com]

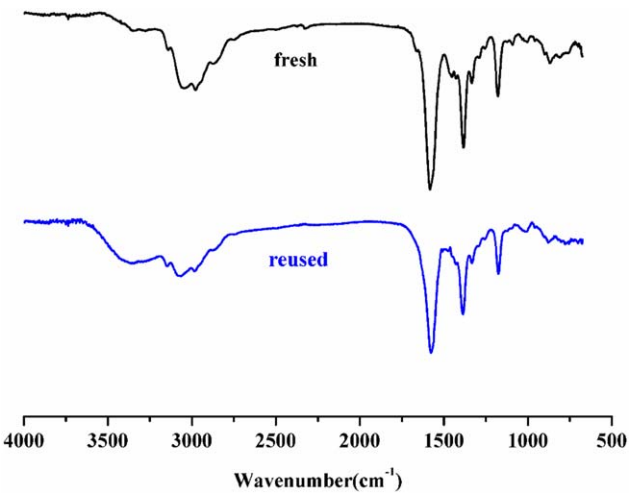

Figure 9. FTIR spectra of fresh and recycled [emim][Gly]+[emim][Ac].

[Color figure can be viewed at wileyonlinelibrary.com]

the same as that of CO_2 absorption in pure AAILs and pure [emim]][Ac].

Recycle of hybrid materials

To evaluate the recyclability of AAIL+[emim][Ac] hybrid materials for CO_2 absorption, CO_2-loaded [emim][Gly]-[emim][Ac] was heated to 353.2 K under a vacuum of 0.001 bar for 6 h, and then reused for the measurement of CO_2 absorption. The absorption-desorption cycles were performed for twelve times. Figure 8 shows the absorption capacities of CO_2 in [emim][Gly]+[emim][Ac] at 313.2 K and 1 bar during the twelve cycles. It can be seen that the absorption of CO_2 in [emim][Gly]+[emim][Ac] is totally reversible, and the absorption capacities of CO_2 remain almost unchanged throughout the twelve cycles. Furthermore, the FTIR spectra of [emim][Gly]-[emim][Ac] after twelve cycles was collected and compared with that of fresh sample, as shown in Figure 9. It is found that there is no obvious change in the characteristic bands of FTIR spectra, demonstrating that the desorption of CO_2 is complete.

Conclusions

In summary, AAIL+[emim][Ac] hybrid materials were proposed as CO_2 absorbents in this work. The rate of CO_2 absorption in AAIL+[emim][Ac] hybrid materials is significantly enhanced in comparison with that in pure AAILs. The viscosity increases of AAIL+[emim][Ac] hybrid materials after CO_2 absorption is much less significant than pure AAILs. Furthermore, the absolute capacities of CO_2 in AAIL+[emim][Ac] hybrid materials still remain at high levels because of the chemical affinity of [emim][Ac]. Therefore, diluting AAILs with [emim][Ac] can not only promote the absorption of CO_2 in AAILs and extend the applicability of AAILs in the industrial capture of CO_2, but also avoid the sacrifice of CO_2 absolute capacities. Based on the results obtained in this work, it is concluded that hybrid materials consisting of a chemical solvent plus another chemical solvent are a class of effective absorbents for the capture of CO_2.

Acknowledgments

This work was supported by National Natural Science Foundation of China (Nos. 21566011, 31570560, 20806037 and 21366019), Natural Science Foundation of Jiangxi Province (Nos. 20151BAB213016 and 20171BAB203019), and Natural Science Foundation of Jiangxi Province for Distinguished Young Scholars (No. 20162BCB23026). K. H. also acknowledges the sponsorship from Nanchang University.

Literature Cited

1. Cox PM, Betts RA, Jones CD, Spall SA, Totterdell IJ. Acceleration of global warming due to carbon-cycle feedbacks in a coupled climate model. *Nature*. 2000;408:184–187.
2. Choi S, Drese JH, Jones CW. Adsorbent materials for carbon dioxide capture from large anthropogenic point sources. *ChemSusChem*. 2009;2(9):796–854.
3. Rochelle GT. Amine scrubbing for CO_2 capture. *Science*. 2009; 325(5948):1652–1654.
4. Zhang XP, Zhang XC, Dong HF, Zhao ZJ, Zhang SJ, Huang Y. Carbon capture with ionic liquids: overview and progress. *Energy Environ Sci*. 2012;5(5):6668–6681.
5. Lei ZG, Dai CN, Chen BH. Gas solubility in ionic liquids. *Chem Rev*. 2014;114(2):1289–1326.
6. Cui GK, Wang JJ, Zhang SJ. Active chemisorption sites in functionalized ionic liquids for carbon capture. *Chem Soc Rev*. 2016;45: 4307–4339.
7. Shiflett MB, Kasprzak DJ, Junk CP, Yokozeki A. Phase behavior of {carbon dioxide plus [bmim][Ac]} mixtures. *J Chem Thermodyn*. 2008;40(1):25–31.
8. Shiflett MB, Yokozeki A. Phase behavior of carbon dioxide in ionic liquids: [emim][Acetate], [emim][Trifluoroacetate], and [emim][Acetate] plus [emim][Trifluoroacetate] mixtures. *J Chem Eng Data*. 2009;54(1):108–114.
9. Yokozeki A, Shiflett MB, Junk CP, Grieco LM, Foo T. Physical and chemical absorptions of carbon dioxide in room-temperature ionic liquids. *J Phys Chem B*. 2008;112(51):16654–16663.
10. Bates ED, Mayton RD, Ntai I, Davis JH. CO_2 capture by a task-specific ionic liquid. *J Am Chem Soc*. 2002;124(6):926–927.
11. Gurkan BE, de la Fuente JC, Mindrup EM, Ficke LE, Goodrich BF, Price EA, Schneider WF, Brennecke JF. Equimolar CO_2 absorption by anion-functionalized ionic liquids. *J Am Chem Soc*. 2010;132(7): 2116–2117.
12. Zhang JM, Zhang SJ, Dong K, Zhang YQ, Shen YQ, Lv XM. Supported absorption of CO_2 by tetrabutylphosphonium amino acid ionic liquids. *Chem Eur J*. 2006;12(15):4021–4026.
13. Zhang YQ, Zhang SJ, Lu XM, Zhou Q, Fan W, Zhang XP. Dual amino-functionalised phosphonium ionic liquids for CO_2 capture. *Chem Eur J*. 2009;15(12):3003–3011.
14. Gurkan B, Goodrich BF, Mindrup EM, Ficke LE, Massel M, Seo S, Senftle TP, Wu H, Glaser MF, Shah JK, Maginn EJ, Brennecke JF, Schneider WF. Molecular design of high capacity, low viscosity, chemically tunable ionic liquids for CO_2 capture. *J Phys Chem Lett*. 2010;1(24):3494–3499.
15. Wang CM, Luo HM, Jiang DE, Li HR, Dai S. Carbon dioxide capture by superbase-derived protic ionic liquids. *Angew Chem Int Ed*. 2010; 49(34):5978–5981.
16. Wang CM, Luo XY, Luo HM, Jiang DE, Li HR, Dai S. Tuning the basicity of ionic liquids for equimolar CO_2 capture. *Angew Chem Int Ed*. 2011;50(21):4918–4922.
17. Luo XY, Guo Y, Ding F, Zhao HQ, Cui GK, Li HR, Wang CM. Significant improvements in CO_2 capture by pyridine-containing anion-functionalized ionic liquids through multiple-site cooperative interactions. *Angew Chem Int Ed*. 2014;53(27):7053–7057.
18. Wang CM, Luo HM, Li HR, Zhu X, Yu B, Dai S. Tuning the physicochemical properties of diverse phenolic ionic liquids for equimolar CO_2 capture by the substituent on the anion. *Chem Eur J*. 2012; 18(7):2153–2160.
19. Kirchhecker S, Esposito D. Amino acid based ionic liquids: a green and sustainable perspective. *Curr Opin Green Sustain Chem*. 2016;2:28–33.
20. Gutowski KE, Maginn EJ. Amine-functionalized task-specific ionic liquids: a mechanistic explanation for the dramatic increase in viscosity upon complexation with CO_2 from molecular simulation. *J Am Chem Soc*. 2008;130(44):14690–14704.
21. Li XY, Hou MQ, Zhang ZF, Han BX, Yang GY, Wang XL, Zou LZ. Absorption of CO_2 by ionic liquid/polyethylene glycol mixture and the thermodynamic parameters. *Green Chem*. 2008;10(8):879–884.
22. Usman M, Huang H, Li J, Hillestad M, Deng L. Optimization and characterization of an amino acid ionic liquid and polyethylene glycol blend solvent for pre-combustion CO_2 capture: experiments and model fitting. *Ind Eng Chem Res*. 2016;55(46):12080–12090.

23. Ma JW, Zhou Z, Zhang F, Fang CG, Wu YT, Zhang ZB, Li AM. Ditetraalkylammonium amino acid ionic liquids as CO_2 absorbents of high capacity. *Environ Sci Technol*. 2011;45(24):10627–10633.
24. Guo BS, Jing GH, Zhou ZM. Regeneration performance and absorption/desorption mechanism of tetramethylammonium glycinate aqueous solution for carbon dioxide capture. *Int J Greenhouse Gas Contro*. 2015;34:31–38.
25. Lv BH, Jing GH, Qian YH, Zhou ZM. An efficient absorbent of amine-based amino acid-functionalized ionic liquids for CO_2 capture: high capacity and regeneration ability. *Chem Eng J*. 2016;289:212–218.
26. Lv BH, Xia YF, Shi Y, Liu N, Li W, Li SJ. A novel hydrophilic amino acid ionic liquid [C_2OHmim][Gly] as aqueous sorbent for CO_2 capture. *Int J Greenhouse Gas Contro*. 2016;46:1–6.
27. Wu ZK, Zhang Y, Lei WK, Yu P, Luo YB. Kinetics of CO_2 absorption into aqueous 1-ethyl-3-methylimidazolium glycinate solution. *Chem Eng J*. 2015;264:744–752.
28. Wu ZK, Huang ZL, Zhang Y, Qin YH, Ma JY, Luo YB. Kinetics analysis and regeneration performance of 1-butyl-3-methylimidazolium glycinate solutions for CO_2 capture. *Chem Eng J*. 2016;295:64–72.
29. Wang XF, Akhmedov NG, Duan YH, Luebke D, Hopkinson D, Li BY. Amino acid-functionalized ionic liquid solid sorbents for post-combustion carbon capture. *ACS Appl Mater Interfaces*. 2013;5(17):8670–8677.
30. Wang XF, Akhmedov NG, Duan YH, Luebke D, Li BY. Immobilization of amino acid ionic liquids into nanoporous microspheres as robust sorbents for CO_2 capture. *J Mater Chem A*. 2013;1(9):2978–2982.
31. Gurau G, Rodriguez H, Kelley SP, Janiczek P, Kalb RS, Rogers RD. Demonstration of chemisorption of carbon dioxide in 1,3-dialkylimidazolium acetate ionic liquids. *Angew Chem Int Ed*. 2011;50(50):12024–12026.
32. Chen FF, Huang K, Zhou Y, Tian ZQ, Zhu X, Tao DJ, Jiang DE, Dai S. Multi-molar absorption of CO_2 by the activation of carboxylate groups in amino acid ionic liquids. *Angew Chem Int Ed*. 2016;55(25):7166–7170.
33. Huang K, Zhang XM, Xu Y, Wu YT, Hu XB, Xu Y. Protic ionic liquids for the selective absorption of H_2S from CO_2: thermodynamic analysis. *AIChE J*. 2014;60(12):4232–4240.
34. Goodrich BF, de la Fuente JC, Gurkan BE, Zadigian DJ, Price EA, Huang Y, Brennecke JF. Experimental measurements of amine-functionalized anion-tethered ionic liquids with carbon dioxide. *Ind Eng Chem Res*. 2011;50(1):111–118.
35. Zhang JZ, Jia C, Dong HF, Wang JQ, Zhang XP, Zhang SJ. A novel dual amino-functionalized cation-tethered ionic liquid for CO_2 capture. *Ind Eng Chem Res*. 2013;52(17):5835–5841.
36. Tian SD, Hou YC, Wu WZ, Ren SH, Qian JG. Reversible absorption of CO_2 by diethylenetriamine hydrochloride and ethylene glycol mixtures with high capacity and low viscosity. *J Taiwan Inst Chem Eng*. 2015;49:95–99.
37. Lee JI, Otto FD, Mather AE. Equilibrium between carbon dioxide and aqueous monoethanolamine solutions. *J Appl Chem Biotechnol*. 1976;26:541–549.
38. Jou FY, Carroll JJ, Mather AE, Otto FD. Solubility of H_2S and CO_2 in aqueous methyldiethanolamine solutions. *J Chem Eng Data*. 1993;38(1):75–77.
39. Besnard M, Cabaco MI, Vaca Chavez F, Pinaud N, Sebastiao PJ, Coutinho JAP, Mascetti J, Danten Y. CO_2 in 1-butyl-3-methylimidazolium acetate. 2. NMR investigation of chemical reactions. *J Phys Chem A*. 2012;116(20):4890–4901.

Manuscript received Feb. 17, 2017, and revision received July 23, 2017.